ESTÁCIO ANTUNES DE OLIVEIRA JÚNIOR

Experimental evaluation of the pressures exerted by maize in slender cylindrical silo using hopper and flat bottom. Comparison with ISO 11697

LAVRAS – MG

2021

ESTÁCIO ANTUNES DE OLIVEIRA JÚNIOR

Experimental evaluation of the pressures exerted by maize in slender cylindrical silo using hopper and flat bottom. Comparison with ISO 11697

Trabalho de conclusão de curso apresentado à Universidade Federal de Lavras – MG, como parte das exigências do curso de Engenharia Agrícola, para obtenção de título de bacharel.

Prof. Dr. Francisco Carlos Gomes
Orientador

M.Sc. Rômulo Marçal Gandia
Coorientador

LAVRAS – MG

2021

ESTÁCIO ANTUNES DE OLIVEIRA JÚNIOR

Experimental evaluation of the pressures exerted by maize in slender cylindrical silo using hopper and flat bottom. Comparison with ISO 11697

Trabalho de conclusão de curso apresentado à Universidade Federal de Lavras – MG, como parte das exigências do curso de Engenharia Agrícola, para obtenção de título de bacharel.

APROVADO em 19 de março de 2021

Prof. Dr. Francisco Carlos Gomes	UFLA
Prof. Dr. Tadayuki Yanagi Júnior	UFLA
M.Sc. Rômulo Marçal Gandia	UFLA

Prof. Dr. Francisco Carlos Gomes
Orientador

M.Sc. Rômulo Marçal Gandia
Coorientador

LAVRAS – MG

2021

RESUMO

Estações de teste em escala piloto possibilita a obtenção de esforços confiáveis e de maneira mais econômica comparado a silos em escalas reais. Portanto, neste trabalho foram avaliadas as pressões normais e de atrito na estação de teste em escala piloto composta por um silo esbelto cilíndrico e metálico utilizando milho, produto de fluxo livre, como produto armazenado. Foram verificados os esforços temporais durante as etapas de carregamento, condição estática e dinâmica. Também foram avaliadas as pressões normais e de atrito máximas. Os resultados foram comparados com a ISO 11697:1995. Durante o enchimento ocorreram picos de acomodação apenas na tremonha α:30°. No geral, as pressões normais foram superiores para o fundo plano e as de atrito superiores para a tremonha α:30°. As máximas pressões experimentais (normais e de atrito) foram inferiores as obtidas na ISO 11697. Portanto, conclui-se que os coeficientes utilizados na norma são suficientes, promovendo segurança nos projetos em silos.

PALAVRAS CHAVE: fluxo de funil, pressões normais, pressões de atrito, milho, silo teste.

ABSTRACT

Pilot scale test stations make it possible to obtain reliable and comparable efforts at full scales following the proposed proportional limits. Therefore, in this work, normal and frictional pressures were evaluated in the test station on a pilot scale test station composed of a slender cylindrical silo using maize, a free-flowing product, as a stored product. Temporal efforts were verified during the filling, static and dynamic conditions. Maximum normal and frictional pressures were also evaluated. The results were compared to ISO 11697: 1995. During filling, accommodation peaks occurred only in the α: 30 ° hopper. In general, normal pressures were higher for the flat bottom and higher frictional pressures for the α: 30 ° hopper. The maximum experimental pressures (normal and friction) were lower than those obtained in ISO 11697. Therefore, it is concluded that the coefficients used in the standard are sufficient, promoting safety in silo projects.

Key Words: funnel flow, normal pressures, frictional pressures, maize, test silo.

SUMÁRIO

1. INTRODUCTION

Brazil's economic growth is influenced by agribusiness, due to the development of productivity in the sector in recent years. In the period from January to October 2020, the participation of agribusiness in PIB was 16.81%, equivalent to 274 billion reais (ESALQ, CEPEA, & CNA, 2021). For the year 2021 it is estimated a production of 256.8 million tons, where maize represents 100.6 million in the first and second harvest (IBGE, 2020). A continental country with a favorable climate for production throughout the year, the agricultural export sector increases annually. With such production, the use of silos for the storage of products is essential, with a static capacity of 171.542 billion tons in 2020 (CONAB, 2020).

However, despite the significant numbers, Brazil does not have its own standard for silo design. Currently, the Brazilian standard is being discussed (CE-203:020.001 – *Comissão de Estudo de Máquinas e Equipamentos para Sistemas de Armazenagem e Beneficiamento de Grãos Vegetais*). The importance of a specific standard is due not only for calculations and structures, it is the history of particularities of the properties of the products stored in the country and the properties of the building materials of the silo, in addition to cultural factors of operation in the storage and climatic conditions.

The study of the behavior of products stored in silos has been dated since 1895 by Janssen (Janssen, 1895). Since then, other theories have been developed (Jenike, Johanson, & Carson, 1973a, 1973b; Walker, 1967; Walters, 1973a, 1973b) supporting international standards (ANSI - American Society of Agricultural and Biological Engineers, 2019; CEN - European Committee for Standardization, 2006; DEUTSCHE NORM, 2005; Internacional Organization for Standardization, 1995).

Most standards classify the product's discharge flow graphically. ISO 11697 uses the hopper angle and the friction angle between the grain and silo wall. The flow can be classified into mass flow or funnel flow and also the intermediate flow (mixed). Mass flow is the most desired and, whenever feasible, the project is dimensioned for that. The advantage of the mass flow promotes a uniform discharge, where all particles are in motion, thus preventing the formation of static zones. In the funnel flow, a channel is formed above the discharge gate, generating static side zones where the product remains stationary (Jenike et al., 1973b, 1973a; JUNIOR & CHEUNG, 2007; Wójcik, Tejchman, & Enstad, 2012).

The flow determination is fundamental for the analysis of the efforts acting on the silo, which are evaluated during the filling and discharge phases. ISO 11697 provides equations for horizontal, vertical and frictional pressures during filling phase in the silo cylinder and hopper. In the case of discharge, efforts are obtained through an overpressure coefficient “C”, which is established according to the slenderness of the silo.

Faced with several studies on failures and collapses in silos (BYWALSKI; KAMIŃSKI, 2019; GUTIÉRREZ et al., 2015; DOGANGUN et al., 2009; SUN; TENG; ZHAO; LAM, 2001; TENG, 1994; TENG; ROTTER, 1989, 1991), it was found that the main causes refer to design errors; on pressures (normal and frictional, on the wall and in the hopper) of the product stored in the structure; excess moisture in the stored product (causing unexpected overpressure); product discharge (maximum pressures in the silo, usually in the silo-hopper transition); discharge eccentricity; temperature variation in the product due to the location of the silo and imperfections in the structural material.

The full-scale experimental model of silos provides proximity to real values, making it possible to understand the pressures in the silos. Worldwide, the number of full-scale experimental silo stations is relatively small (SUN et al., 2020; COUTO; RUIZ; AGUADO, 2012; HÄRTL et al., 2008; RAMÍREZ; NIELSEN; AYUGA, 2010) due to the cost construction, instrumentation and operations. In addition, the scale factor is extremely important for reliable data (BROWN & NIELSEN, 1998). Furthermore, the study of experimental pressures in silo allows advances in numerical studies as a means of validation and comparisons in order to make the models reliable.

The pilot scale test station proposed by Pieper and Schütz in 1980 (Pieper & Schütz, 1980) which helped to base DIN 1055-6: Basis of design and actions on structures - Part 6 (DEUTSCHE

NORM, 2005) allows to evaluate numerous variables that directly influence the behavior of the pressures in the silo with use of any product as long as the maximum diameter of the product is less than 1.7 centimeters (to be allowed proportional to the scale real) (BROWN & NIELSEN, 1998; Pieper & Schütz, 1980); three walls with different roughness (varying the friction coefficient between the product and the wall); twelve height / diameter ratios; 8 bottoms (1 flat bottom, 4 concentric hoppers (α: 75 to 30º) and 3 100% eccentric hoppers with (α: 75 to 45º)) and other possible procedural variables in the tests.

Through catalogs of the main silos' manufacturers in Brazil (GSI, PAGÉ and Kepler Weber) it was noticed that the models of silos sold for the storage of maize and soybeans have flat bottoms or hoppers with beta 45 and 60 ° degrees and maximum H / ratio D = 3. Flat-bottom silos are widely used as they allow better use of their storage volume, ease of handling and lower cost (JUNIOR & CHEUNG, 2007). When using the flat bottom, it is necessary to use labour or mechanical systems to remove the remaining product at the bottom of the silo after discharge, a situation that may not occur when using an inclination in the discharge base (hopper).

Due to the economic importance of maize, the uncertainties in silos pressures and the high number of slender silos and funnel flow silos, this work aims to contribute with information to the Brazilian standard. In addition, the objective of this article was to evaluate the pressures experimentally using maize, free flow product, in slender silo varying the hopper and the flat bottom, and to compare the values obtained with ISO 11697.

2. MATERIAL AND METHODS

2.1. GENERAL DESCRIPTION OF THE INSTALLATION

The tests were conducted in the test station located at the Federal University of Lavras (UFLA) in the Laboratório de propriedades físicas e de fluxo de produtos armazenados. The station (Figure 1) consists of a stored silo where the product to be tested is stored, a bucket elevator that transports the material and an instrumented pilot silo for pressure analysis.

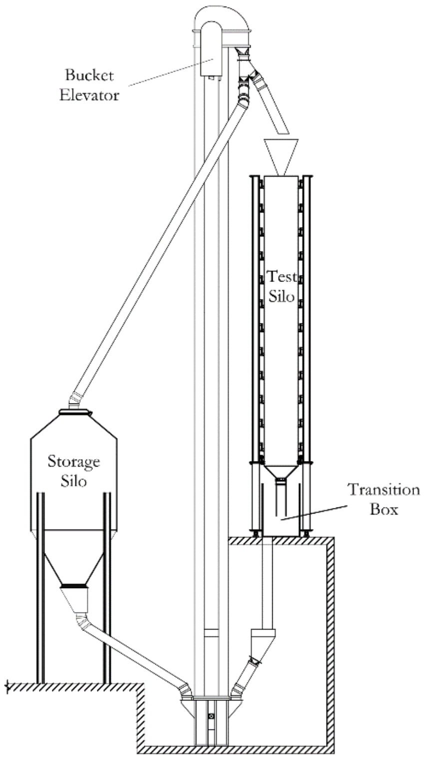

FIGURE 1. Pilot silo test station.

2.2. GEOMETRY OF PILOT SILO

The pilot silo has a total height of six meters and is subdivided into 12 independent and suspended rings, with a height of 495 mm and an internal diameter of 688 mm. The silo wall is made of smooth galvanized steel with a thickness of 10 mm, designed to ensure that the efforts made during the tests are transferred to the wall without deformation of the same.

Each ring has a vertical cut with a spacing of 5 mm in the gap between the rings, which guarantees structural interdependence. The instrumentation of each ring was performed with two pairs of traction load cells. The first pair are located in the center and perpendicular to the vertical opening of the ring, determining the horizontal pressure on the wall, which in its normal state will be pre-tensioned with three helical springs, making the set more sensitive to efforts (Figure 2). The second pair is located next to the outer wall of the ring and fixed using clamps articulated to the pillars of the silo, indicating the vertical acting force (Figure 2).

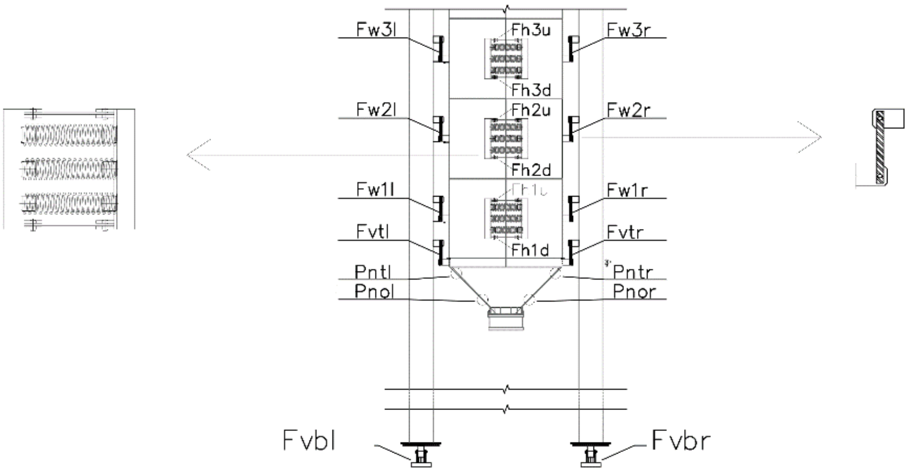

FIGURE 2. Location of measurement cells.

The rings are suspended and supported by three pillars, where one of them only has the function of stabilizing them so that they do not promote rotation. The other two have at their base a beam load cell with a capacity of 50 kN, which, from the sum of the load of the two pillars, it is possible to obtain the weight of the stored product (Figure 4).

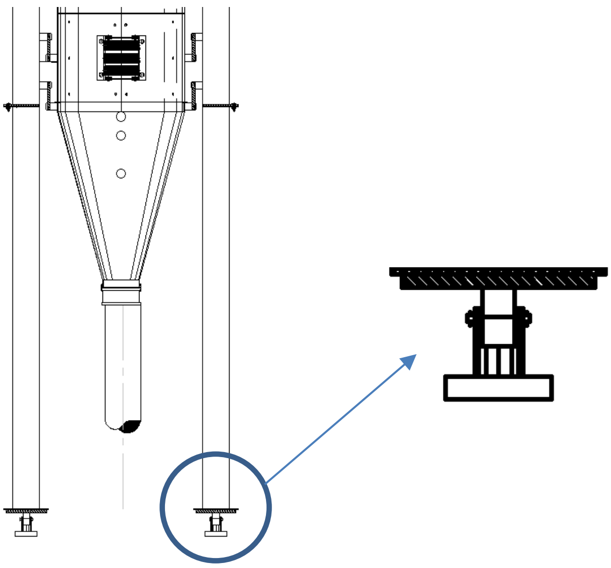

FIGURE 4. Support pillars and location of beam load cells.

The station has four hoppers with concentric discharge (α: 30 °, 45 °, 60 ° and 75 °), three eccentric hoppers (α: 45 °, 60 ° and 75 °) and a flat bottom with concentric discharge. The α: 30 ° hopper and the flat bottom used in this study are instrumented with four pressure cells distributed and attached to their wall as shown in Figure 5.

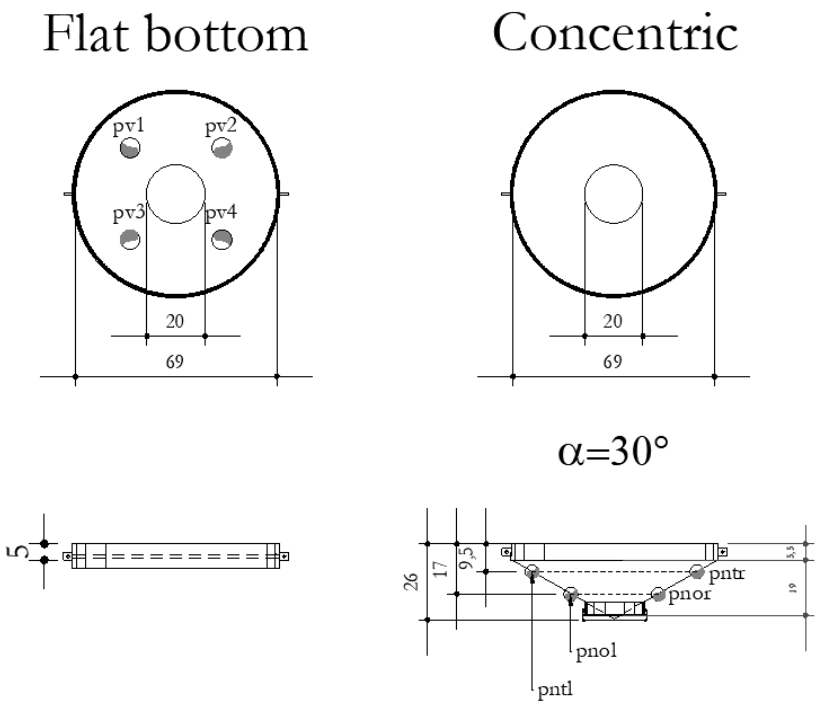

FIGURE 5. Hopper geometry and positioning of pressure cells.

In the transition, the hoppers are connected to the support pillars by a set of clamp and traction load cell, which have articulated connections at both ends and are connected through a stainless-steel pin. The same system used in the vertical support of each ring (Figure 2).

The acquisition of electrical signals (mV / V) was performed by a module, model DS2000 from the manufacturer LYNX, with a capacity for 64 channels and a maximum frequency of 65.5 kHz. The calibration and treatment of the data were performed using the Aqdados software (version 7.5) from the same manufacturer.

2.3. DESCRIPTION OF TESTS

The determination of the physical characteristics of the maize was conducted out at the Centro de Tecnologia e Recursos Naturais da Universidade Federal de Campina Grande (UFCG), using Jenike's shear device (Jenike Shear Cell) (WPMPS, 1989).

Pressure analysis was performed during the filling, static and discharge. The filling height of the product was 1.50 meters, the height / diameter ratio was 2.18. The acquisition system was configured to collect data at a frequency of 2Hz. The test variables were two bottoms: α hopper: 30 °

and flat bottom, both with concentric discharge. For each variable, three repetitions were performed, totaling six complete tests.

The maize was transported to the pilot silo through a bucket elevator with constant flow and centralized filling, until the moment when the grain mass reached close to the height of 1.5 meters from the transition. After filling, it was waited 10 min (static condition) to stabilize the system and accommodate the stored product.

At the discharge, the hopper gate was completely opened, promoting a free discharge, where the highest pressure is expected in this stage. After opening the discharge gate, the maize fell into the transition box for do not exceed the bucket elevator carrying capacity. From the bucket elevator, the product is taken to the stored silo, finishing the test (Figure 7)

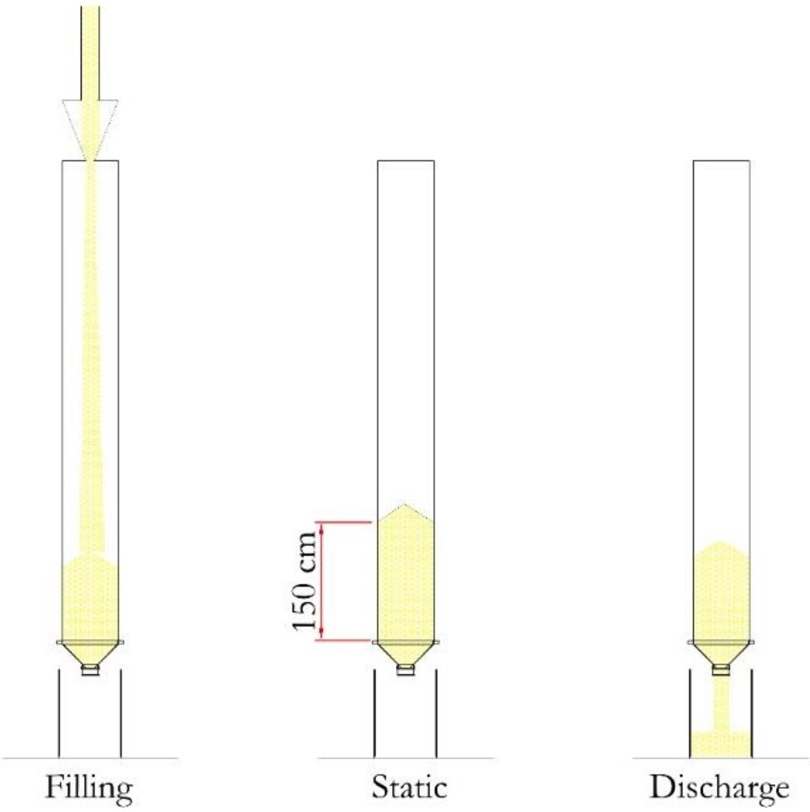

FIGURE 7. Testing stage: Filling, static and discharge.

According to the ISO 11697 (Internacional Organization for Standardization, 1995), flow characterization (Available at ISO “Figure 2 - Limit between mass flow and funnel flow for circular hoppers"), the friction coefficient of the tested maize was used (7.38 – 9.23) and 30º hopper and flat bottom the material will be discharged with funnel flow.

3. RESULTS AND DISCUSSION

In order to expose the uniformity between the repetitions of the tests and the difference between the two configurations, Table 1 presents the average values of loading (weight of the stored product) during the filling and discharge phases in the pilot silo.

TABLE 1. Product weight.

	Average value (kN)		Standard deviation (%)	
	Filling	Discharge	Filling	Discharge
Concentric (α = 30°)	5.4	5.5	7.3	7.4
Flat Bottom	5.1	5.0	3.4	3.9

With this information it is possible to affirm that the repetitions between each configuration presented low variability (statistically equal). It is also possible to state that the two configurations differ due to the greater volume of the 30 ° hopper.

To reinforce that the tests were subjected to approximate test conditions, Table 2 shows the average of the times in each phase of the tests.

TABLE 2. Trial time

	Average value (s)			Standard deviation (%)		
Test	Filling	Static	Discharge	Filling	Static	Discharge
Concentric (α = 30°)	189.0	646.2	47.2	8.9	2.3	27.5
Flat Bottom	189.3	631.5	34.8	3.0	1.6	30.4

It is possible to observe a considerable deviation in the discharge phase, caused by turbulence and complexity in the flow. Once again, to reinforce the same test conditions and compare the discharge flow between the two configurations, the flow rate in the filling and discharge phase was calculated (Table 3).

TABLE 3. Average flow rate for each test.

Test	Average value (Kg/s)		Standard deviation (%)	
	Filling	Discharge	Filling	Discharge
Concentric (α = 30°)	2.9	12.8	1.9	38.3
Flat Bottom	2.8	15.7	5.6	36.6

The filling flow rate, in addition to having a relatively low deviation between repetitions, is statistically equal between the two configurations. As expected, the discharge rate is higher. The deviation between repetitions is relatively greater than in filling due to the funnel flow pattern (Internacional Organization for Standardization, 1995), showing random behavior during the discharge phase (Jenike et al., 1973b; JUNIOR & CHEUNG, 2007).

This work generated a large volume of data. Therefore, to avoid exposing unnecessary data, Table 4 and Table 5 present the average values in each measurement cell referring to the pilot silo instrumentation for configuring the 30 ° concentric hopper and flat bottom respectively in the three phases

TABLE 4. Mean pressure values in the hopper configuration (α = 30).

Sensor	Load (kPa)			Standard deviation (%)		
	Filling	Static	Discharge	Filling	Static	Discharge
ph3	0.78	0.91	1.55	19.97	15.25	11.12
ph2	1.70	1.92	2.81	15.41	11.50	6.82
ph1	2.95	3.32	3.43	3.32	9.49	3.19
pntr	1.17	1.27	11.16	17.15	25.80	15.56

pntl	1.71	1.21	10.88	19.11	29.72	14.82
pnor	5.87	6.42	5.23	12.49	9.21	10.83
pnol	4.55	4.96	4.88	15.09	17.92	16.70
pvt	10.20	10.67	10.07	3.85	3.00	2.29
pw3	0.21	0.30	0.40	7.35	4.76	9.40
pw2	0.47	0.55	0.65	18.01	7.85	3.99
pw1	1.06	1.08	1.13	13.34	11.44	10.55

TABLE 5. Mean pressure values in the flat bottom configuration.

	Load (kPa)			Standard deviation (%)		
Sensor	Filling	Static	Discharge	Filling	Static	Discharge
ph3	0.91	0.90	1.55	44.37	45.80	39.04
ph2	2.50	2.51	2.81	6.89	6.65	6.51
ph1	3.82	3.82	4.34	4.67	4.86	2.87
pv1	7.84	7.93	8.11	10.72	10.07	7.54
pv2	7.30	7.44	8.43	6.90	6.08	3.19
pv3	8.93	9.04	9.41	9.51	9.28	8.40
pv4	5.68	5.79	6.71	1.72	2.50	8.04
pvt	10.34	10.33	9.59	2.74	2.81	4.88
pw3	0.18	0.22	0.36	11.93	11.51	22.22
pw2	0.45	0.50	0.61	2.17	1.53	12.78
pw1	0.95	0.95	0.86	3.37	3.18	9.30

One of the three repetitions of each configuration will be showed (chosen at randomly). The results show the pressures for three regions of the silo: cylinder (normal pressures and friction), transition (tension of the product stored in the transition) and flat or hopper bottom (normal pressures). The analysis of the results was discussed in the three phases: filling, static condition and discharge.

CONCENTRIC (α = 30°)

The temporal analysis of the behavior of normal pressures in the silo with a hopper α = 30 ° during the three phases is shown in Figure 8.

FIGURE 8**.** Normal pressures on the silo wall (ph, i; pnt; pno), vertical stress in the stored material at the transition (pvt) and the weight of the stored material (W) using hopper α = 30 °.

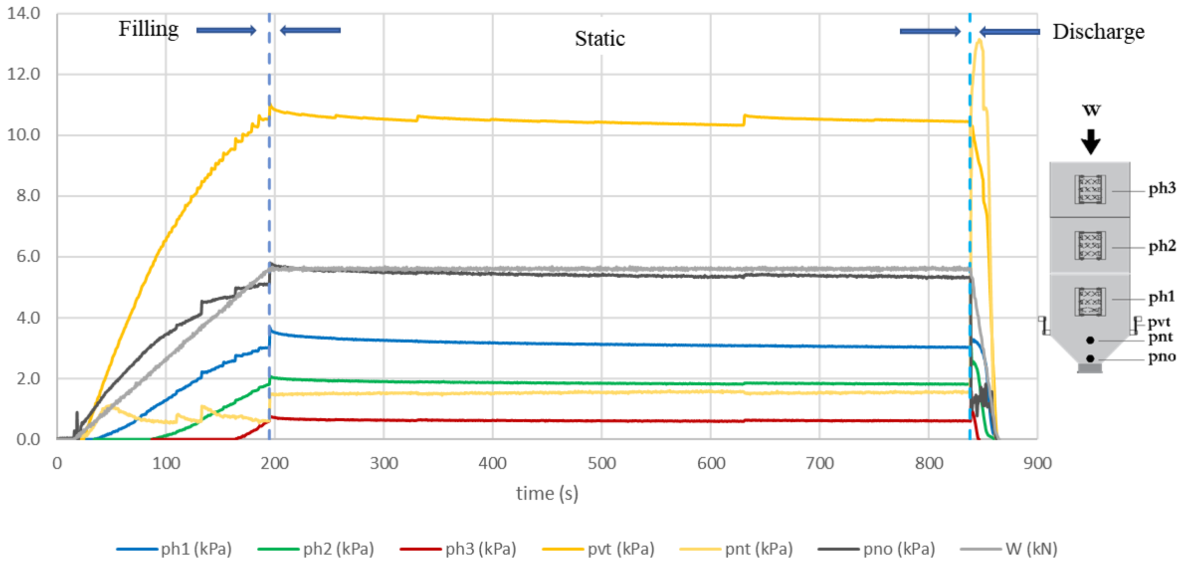

There is an increase in pressure near the hopper outlet (pno) in the first seconds of filling, explained due to the height of the product falling to the bottom of the silo (6 meters). The weight of the stored product (W) does not vary as the pressures, so it presents a linear behavior throughout the test, allowing to obtain the flow rate in the filling and discharge steps (Table 3).

The maximum pressure occurred in the silo-hopper transition (pnt) shortly after the beginning of the discharge of the product (Internacional Organization for Standardization, 1995), besides being a well-known foundation (Härtl et al., 2008; Ramírez, Nielsen, & Ayuga, 2010b). The frictional pressures were obtained in the cylinder and are shown in Figure 9.

FIGURE 9**:** Friction pressures on the silo wall (pw, i) using hopper α = 30 °.

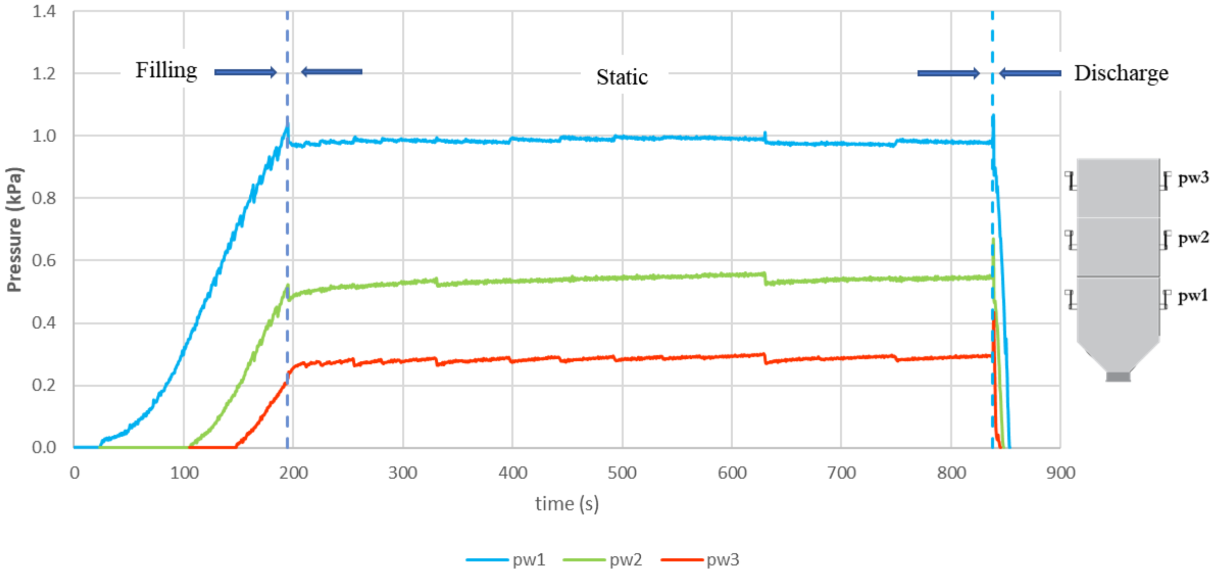

As seen in Figure 8, Figure 9 also reinforces the quality of the instrumentation. During the filling, the beginning of the measurements in each of the rings is observed, with temporal intervals that reinforce the precision in the instrumentation. In addition, during the static phase, it is easy to observe the peaks related to the accommodation of the material, which are synchronous in all measurement cells, regardless of whether they are pressure or load cell.

Another observation related to the static phase is related to vertical stress in the stored material at the transition (pvt) and the friction pressures in the cylinder (pwi). It is observed that while frictional pressures show decreasing accommodation peaks, vertical stress in the stored material at the transition (pvt) shows increasing accommodation peaks. In other words, while the stored product accommodates and tends to move slightly vertically, decreasing the frictional force in the cylinder, simultaneously there is an increase in vertical stress in the stored material at the transition (pvt) due to the increase in the vertical pressure provided by the movement of the stored product.

FLAT HOPPER

The temporal analysis behavior of normal pressures in the flat bottom silo during the three phases is shown in Figure 10.

FIGURE 10: Normal pressures on the silo wall (ph, i; pnt; pno), vertical stress in the stored material at the transition (pvt) and the weight of the stored material (W) using flat bottom.

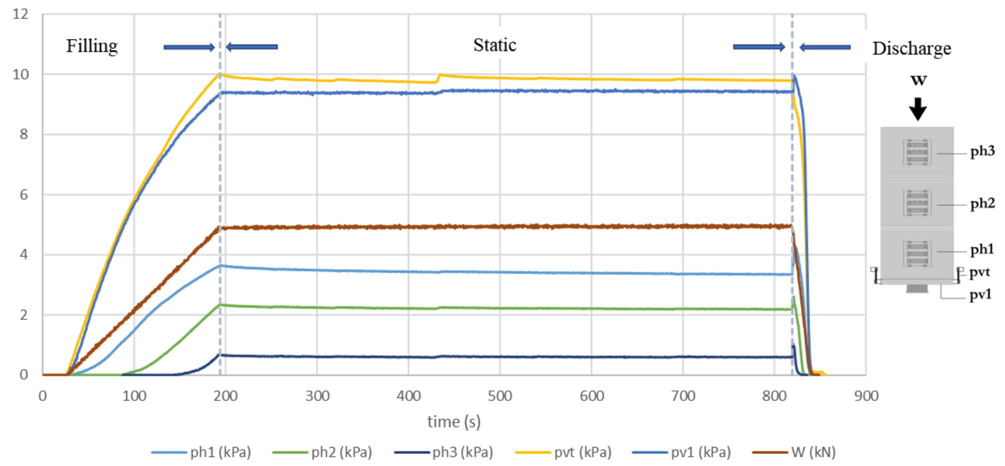

The filling phase for a flat bottom differs from the α = 30 ° hopper, as no accommodation peaks are observed during filling for the flat bottom. The reason is that with the hopper α = 30 ° the material is destabilized at the bottom of the silo due to the inclination of the hopper, promoting the accommodation of the material during filling, unlike the flat bottom, the material stabilizes and there is no such accommodation.

As predicted, normal pressure at the bottom (pv1) is very similar to vertical stress in the stored material at the transition (pvt). In general, the normal pressures in the cylinder in the filling and static phase are higher with the lowest inclination of the hopper, in this case flat bottom. Therefore, it is observed that on the flat bottom the pressures are greater than those of the hopper α = 30 °, however, in the discharge, the opposite occurs, greater pressure peaks with greater inclinations (CEN - European Committee for Standardization, 2006; Internacional Organization for Standardization, 1995; Jenike, 1964; Jenike et al., 1973a; Wójcik et al., 2012). Frictional pressures can be seen in Figure 11: Friction pressures on the silo wall (pw, i) using flat bottom.

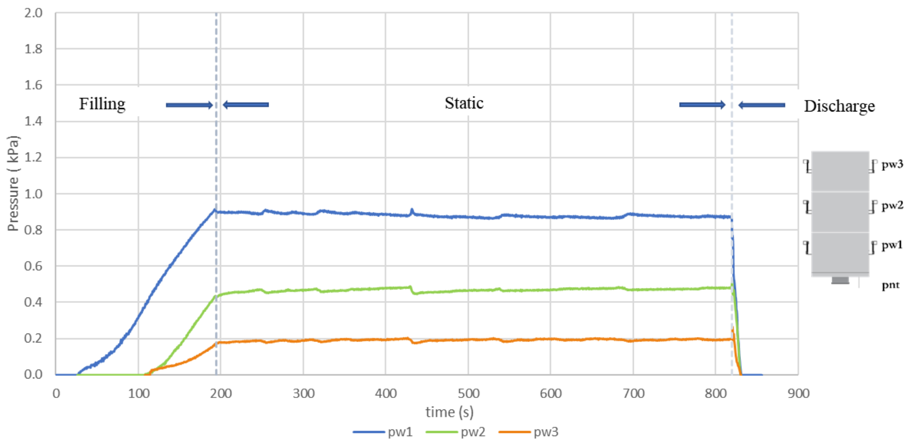

Once again it was possible to observe the quality of the instrumentation by the time intervals during the filling in the rings and also by the synchrony in the accommodation peaks during the static phase. The friction pressure in ring 3 (pw3) was observed to start the measurement at the same time as ring 2 (pw2). The possible reason is the dissipation of the product in the discharge due to the slenderness of the pilot silo, promoting the beginning of the vertical force at the height of ring 3 before the grain mass reaches its level.

As previously mentioned for the friction pressure (pwi) and the vertical stress in the stored material at the transition (pvt) has the same behavior during the static phase of what happened for hopper α = 30 °.

FILLING

In filling, pressures had different time patterns. In Figure 12 and Figure 13 the normal pressures up to the height of 1.50 meters and the vertical stress in the stored material at the transition (pvt) are shown for the hopper α = 30 ° and the flat bottom respectively.

FIGURE 12. Filling pressures, α hopper: 30 °.

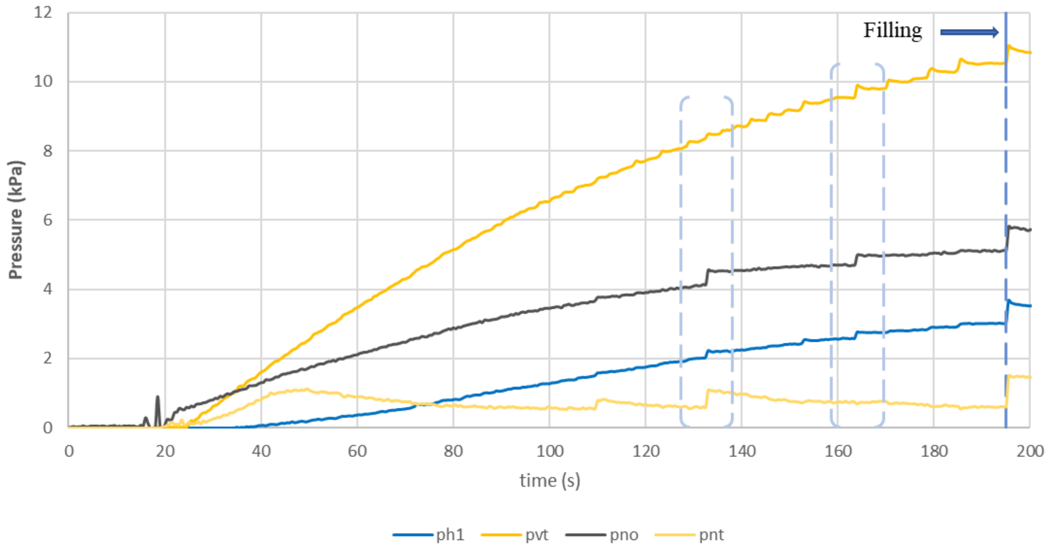

The fluctuations in the accommodation of the material during filling due to the inclination of the hopper are seen in Figure 12. The greater the height of the product in the silo (the greater the weight of the grain mass), the greater the magnitude of the accommodation peaks, at 126.5 and 171 seconds and also when the filling is completed. The behavior of pressures on the flat bottom occurs in a different way (Figure 13).

FIGURE 13**:** Filling pressures, flat bottom.

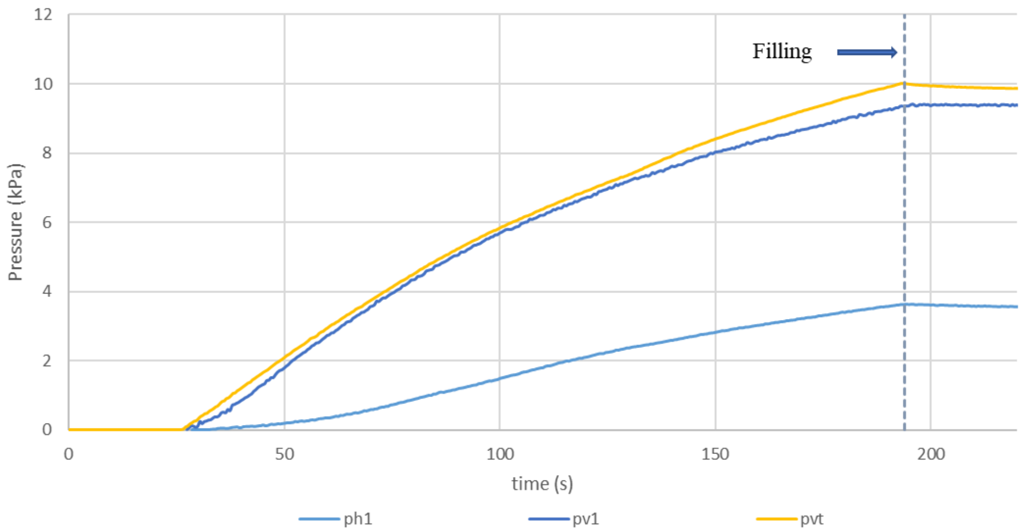

As explained above, due to the stabilization provided by the flat bottom (90 ° angle) the pressures do not fluctuate.

STATIC

The observations regarding the non-linearities of the material pressures during the static condition, that is, the accommodation, were discussed first time in 2012 (Couto, Ruiz, & Aguado, 2013; Ruiz, Couto, & Aguado, 2012). Figure 14 and Figure 15 show a better visualization of the static condition regarding the normal and frictional pressures in the silo for the hopper α = 30 ° and the flat bottom, respectively.

FIGURE 14. Pressures in static condition, hopper α: 30 °.

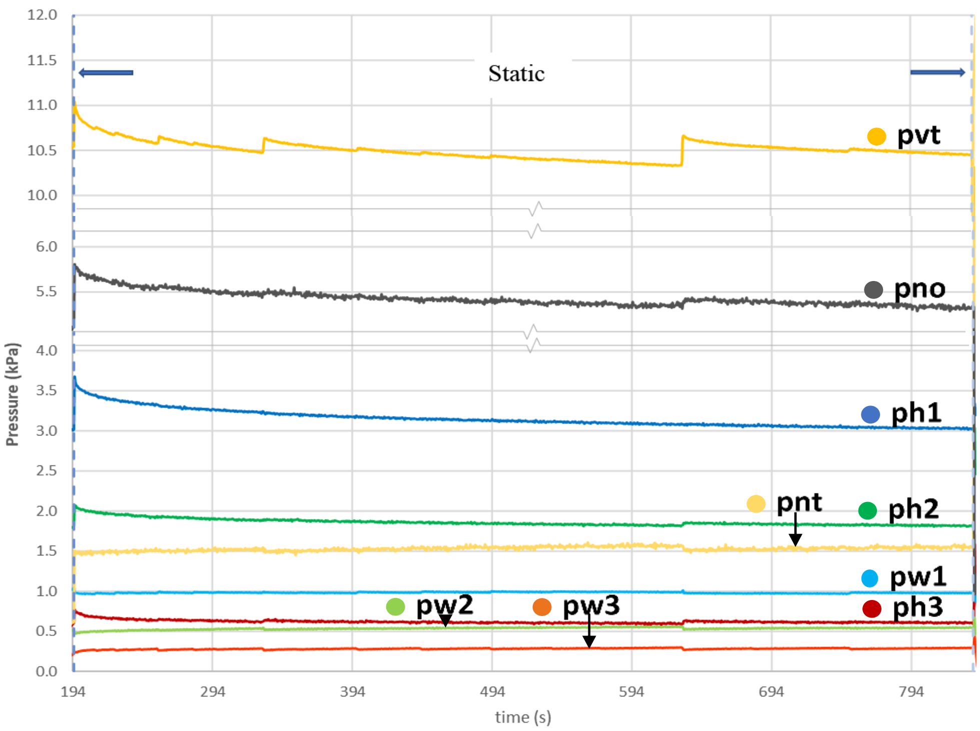

FIGURE 15. Pressures in static condition, flat bottom.

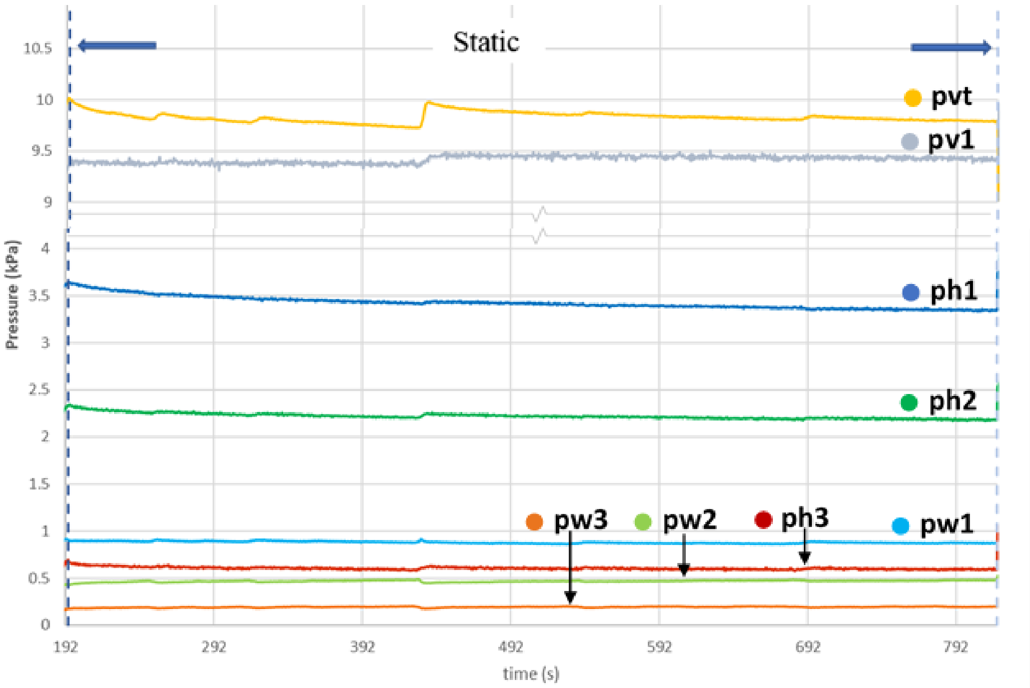

It was observed in Figure 14 and Figure 15, and found by the authors mentioned above, that after filling the silo, the frequency of accommodation peaks is high and decreases over time. This is influenced by the segregation of the material, variation in the specific weight of the material along the height of the silo and the angle of friction between the product and the silo wall and also angle of friction of the stored product.

In this work it can be seen that the magnitude of the peaks is greater for the hopper α: 30 °. Than for the flat bottom, reinforcing the statement during the filling about the destabilization of the stored product due to the inclination of the hopper.

It is also noted that while normal pressures (ph, i; pnt; pno) oscillated upward, frictional pressures behaved in an inverse way. The material tends to compact by moving vertically (releasing frictional stresses) and expanding the normal stresses on the cylinder and hopper.

Discharge

As expected, maximum stresses occur during material discharge (Couto, Ruiz, Herráez, Moran, & Aguado, 2013; Jenike et al., 1973b; Sadowski, Michael Rotter, & Nielsen, 2020; Sadowski & Rotter, 2011). It is known that for funnel flow, flow defined in this paper (Internacional Organization for Standardization, 1995) the maximum pressures also occur, despite being less than the mass flow (Jenike et al., 1973b, 1973a; Wójcik et al., 2012). The pressures in the silo cylinder are shown in Figure 16. Discharge efforts are between 838 and 864 seconds from the start of the test.

FIGURE 16. Discharge normal and frictional in cylinder pressures, α hopper: 30 °.

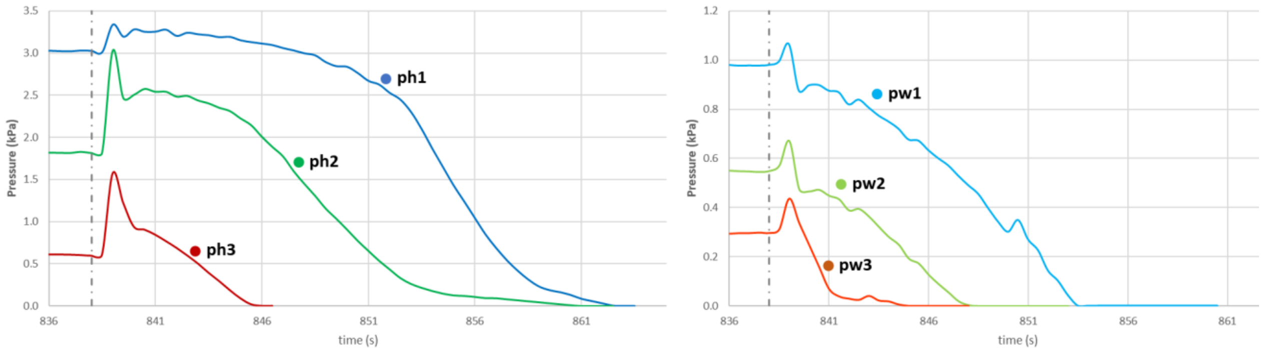

An increase in pressures (friction and normal) was observed in the entire cylinder. The flow channel is supposed to be in the middle of the first ring (ph1 and pw1) and as soon as the discharge started, the volume of the hopper product was displaced and there was a small pressure peak proportional to the displaced volume. The second ring (ph2 and pw2) had the highest pressure peak, admitting the absence of a static zone and a greater volume of stored product than the third ring, providing greater pressure. The third ring (ph3 and pw3), with less volume of stored product and absence of flow channel, presenting overpressure lower than that of the second ring.

FIGURE 17. Discharge normal in hopper and vertical pressures, α hopper: 30 °.

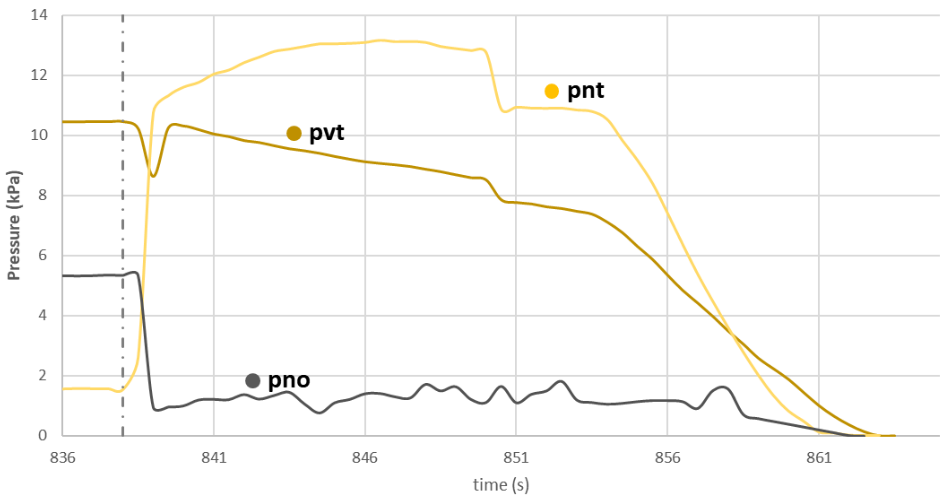

The magnitude of the normal over pressure in the silo-hopper transition is already well defined in norms and theories (CEN - European Committee for Standardization, 2006; Couto, Ruiz, & Aguado, 2013; Couto, Ruiz, Herráez, et al., 2013; Internacional Organization for Standardization, 1995; Jenike et al., 1973b, 1973a), therefore, pnt presented the greatest pressure under the discharge. Mass flow has higher pressures compared to incident flow (funnel)(Jenike et al., 1973b; Wójcik et al., 2012), however, it remains the maximum pressure point in the silo because the state of the stored material changes (static to dynamic).

The pressure drop that occurs in pvt is due to the relief caused by the beginning of the flow and the movement of the stored product, being related to the height of the stored product and the inclination of the hopper. This pressure is resumed instantly, since from the moment the volume of the stored product is moved below the transition plane, this space is quickly filled and the pressure is transmitted again to the transition plane.

The efforts on the flat bottom in the discharge, occur between the times of 819 and 843 seconds from the beginning of the test (Figure 18 and Figure 19).

FIGURE 18. Discharge normal and frictional in cylinder pressures, flat bottom.

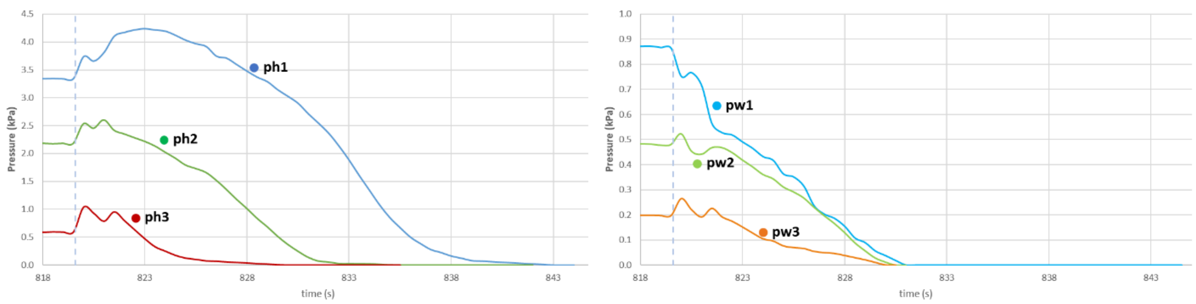

It is observed (Figure 18) that just after the discharge the magnitude of the overpressures is inversely proportional to the height of the silo, in other words, ph1 <ph2 <ph3. However, the normal pressure in the first ring (ph1) continues to increase. The possible reason is the collapse of the flow channel formed in the cylinder, causing the pressures over time until the volume stabilizes and the pressures decrease.

The frictional temporal pressure in the first ring (pw1) behaves differently from the others. A decrease in pressure is visualized at the beginning of the flow, reinforcing the affirmation of the presence of the volume of stored product stagnated in that region (flow channel), occurring less flow, therefore less vertical force in the region of the first ring.

The vertical pressures at the bottom of the silo (pv1) and the vertical stress in the stored material at the transition (pvt), exhibit the same behavior due to their proximity.

FIGURE 19. Discharge vertical pressures, flat bottom.

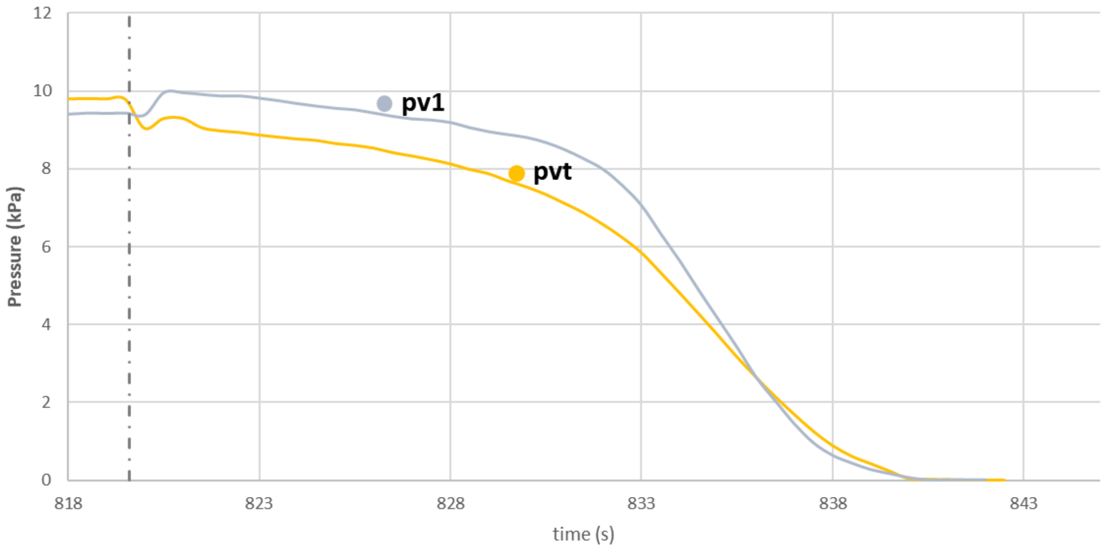

The behavior of the pressures in Figure 19 allow to infer that there was formation of a flow funnel (static zone), since there was no significant increase in pressure in the discharge, characterizing the flow of the funnel (Jenike et al., 1973b).

MAXIMUM PRESSURE

The maximum normal and frictional experimental pressures for both test configurations (α: 30 ° hopper and flat bottom) are plotted and compared to ISO 11697: 1995 (Figure 20 and Figure 21).

FIGURE 20. Maximum experimental and ISO pressures, α hopper: 30 °.

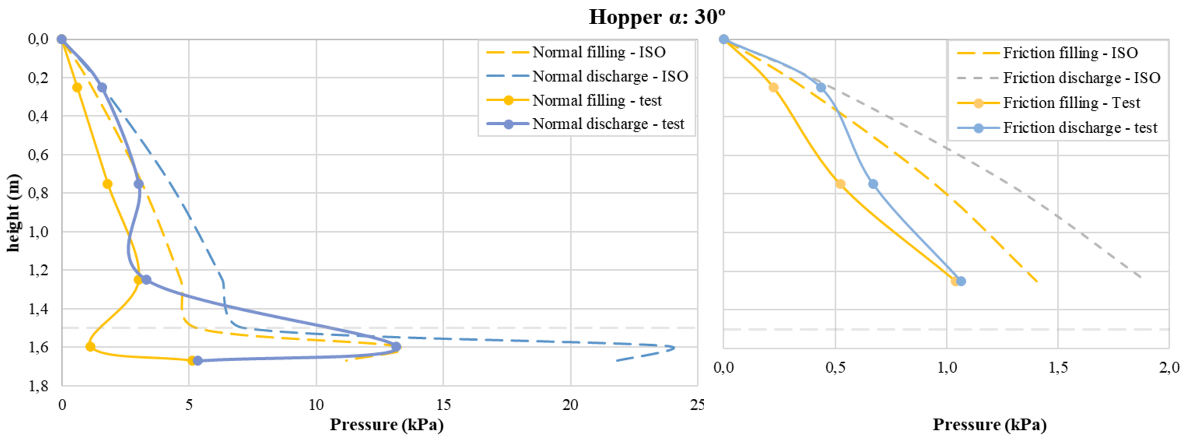

Experimental pressures were lower than those of ISO (Internacional Organization for Standardization, 1995). In order to obtain pressures by the standard, a 35% “C” overpressure coefficient is used due to the slenderness of the cylinder, in addition to the “ps” coefficient that suggests an increase of 2 * ph0 (where ph0 is the horizontal filling pressure in the paralel section) over an inclined distance de 0.2 * diameter of silo below the transition.

In the results obtained, it was noted that the experimental pressure is 53% lower than that calculated by the Standard in the first ring (ph1) above the transition and 55% in the transition region (pnt). Demonstrating the increase coefficient of the experimental pressures, aiming to provide security to the projects.

For flat bottom silo, the ISO indicates the use of the “C” overpressure coefficient related to slenderness, which remained at 35%. In addition to this coefficient, an empirical safety factor of 35% must also be applied increase in vertical pressure during the filling and discharge phases.

FIGURE 21. Maximum experimental and ISO pressures, flat bottom.

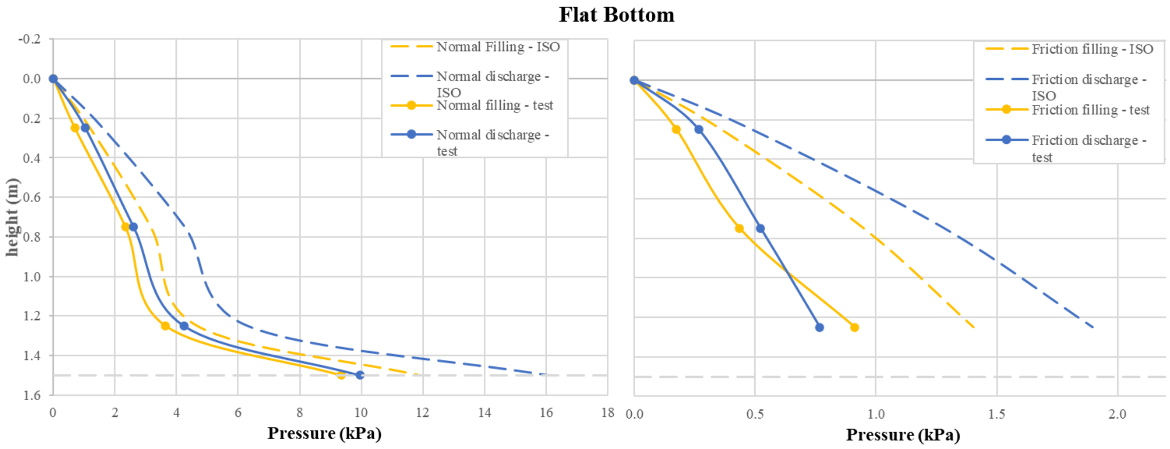

The experimental pressures at the transition of the silo were lower than those obtained by the standard, increasing by 22% in the filling and 38% in the discharge, demonstrating that the safety factors are sufficient to guarantee the results obtained in this study.

A different situation than expected occurred in the frictional pressures, where the maximum pressures occurred in the filling and not in the discharge, this was due to the height of the effective transition having passed ring one. But both still remained below standard.

4. CONCLUSIONS

During filling, pressures in the α: 30 ° hopper showed accommodation peaks due to the instability caused by the hopper inclination, different from what happened on the flat bottom that did not show oscillations in this stage. The pressures were not constant in the static condition, presenting greater variability in the friction pressures, both in the flat bottom and in the α: 30 ° hopper.

Normal cylinder pressures, in general, were higher for the flat bottom, which was to be expected. The frictional pressures in the cylinder were higher for the α: 30 ° hopper.

At discharge, as expected, maximum pressures (normal and frictional) occurred in the cylinder in both cases (flat bottom and α hopper: 30 °). The maximum pressures in the silo-hopper transition of the product discharge stage were obtained only for the α: 30 ° hopper, different from the flat bottom.

The maximum normal pressures in the hopper cylinder α: 30 ° were approximately half that proposed by ISO 11697. For the flat bottom, the vertical experimental pressures at the transition were

38% less than the values obtained in ISO 11697, providing safety in silo projects. In both cases, the frictional pressures on the cylinder were lower than normal.

5. REFERENCES

ANSI - American Society of Agricultural and Biological Engineers. (2019). *Loads Exerted by Free-Flowing Grain on Bins. ANSI/ASAE*. St Joseph.

Brown, C. J., Lahlouh, E. H., & Rotter, J. M. (2000). Experiments on a square planform steel silo. *Chemical Engineering Science*, *55*(20), 4399–4413. doi: 10.1016/S0009-2509(99)00574-6

BROWN, C. J., & NIELSEN, J. (1998). *Silos: Fundamentals of theory, behaviour and design* (E & FN Spon, ed.). London.

Bywalski, C., & Kamiński, M. (2019). A case study of the collapse of the over-chamber reinforced concrete ceiling of a meal silo. *Engineering Structures*, *192*(March), 103–112. doi: 10.1016/j.engstruct.2019.04.100

CEN - European Committee for Standardization. (2006). *EN 1991-4:2006. Eurocode 1: Actions on Structures. Part 4: Silos and Tanks*. Brussels.

Couto, A., Ruiz, A., & Aguado, P. J. (2012). Design and instrumentation of a mid-size test station for measuring static and dynamic pressures in silos under different conditions - Part I: Description. *Computers and Electronics in Agriculture*, *85*, 164–173. doi: 10.1016/j.compag.2012.04.009

Couto, A., Ruiz, A., & Aguado, P. J. (2013). Experimental study of the pressures exerted by wheat stored in slender cylindrical silos, varying the flow rate of material during discharge. Comparison with Eurocode 1 part 4. *Powder Technology*, *237*, 450–467. doi: 10.1016/j.powtec.2012.12.030

Couto, A., Ruiz, A., Herráez, L., Moran, J., & Aguado, P. J. (2013). Measuring pressures in a slender cylindrical silo for storing maize. Filling, static state and discharge with different material flow rates and comparison with Eurocode 1 part 4. *Computers and Electronics in Agriculture*, *96*, 40–56. doi: 10.1016/j.compag.2013.04.011

DEUTSCHE NORM. (2005). *DIN 1055-6: Basis of design and actions on structures – Part 6: design 623 loads for buildings and loads in silo bins*. Berlin, Verlaz.

Dogangun, A., Karaca, Z., Durmus, A., & Sezen, H. (2009). Cause of damage and failures in silo structures. *Journal of Performance of Constructed Facilities*, *23*(2), 65–71. doi: 10.1061/(ASCE)0887-3828(2009)23:2(65)

ESALQ, CEPEA, & CNA. (2021). PIB DO AGRONEGÓCIO AVANÇA NOVAMENTE EM OUTUBRO.

Gutiérrez, G., Colonnello, C., Boltenhagen, P., Darias, J. R., Peralta-Fabi, R., Brau, F., & Clément, E. (2015). Silo collapse under granular discharge. *Physical Review Letters*, *114*(1), 5–9. doi: 10.1103/PhysRevLett.114.018001

Härtl, J., Ooi, J. Y., Rotter, J. M., Wojcik, M., Ding, S., & Enstad, G. G. (2008). The influence of a cone-in-cone insert on flow pattern and wall pressure in a full-scale silo. *Chemical Engineering Research and Design*, *86*(4), 370–378. doi: 10.1016/j.cherd.2007.07.001

IBGE. (2020). *Levantamento Sistemático da Produção Agrícola - Estatística da Produção Agrícola*.

Internacional Organization for Standardization. (1995). *ISO 11697:1995. Bases for design of strutures - Loads due to bulk materials*.

Janssen, H. A. (1895). Versuche uber getreidedruck in silozellen. *Z. Ver. Dtsch. Ing*, *39*(35), 1045–1049.

Jenike, A. . (1964). *Storage and Flow of Bulk Solids Bull. 123*. University of Utah, USA.

Jenike, A. W., Johanson, J. R., & Carson, J. W. (1973a). Bin loads—part 3: mass-flow bins. *Journal of Manufacturing Science and Engineering, Transactions of the ASME*, *95*(1), 6–12. doi: 10.1115/1.3438163

Jenike, A. W., Johanson, J. R., & Carson, J. W. (1973b). Bin Loads—Part 4: Funnel-Flow Bins. *Journal of Engineering for Industry*, *95*, 13–20.

JUNIOR, C. C., & CHEUNG, A. B. (2007). *Silos: pressões, fluxo, recomendações para o projeto e* *exemplo de cálculo* (SET/EESC-USP, Ed.). São Carlos.

Pieper, K., & Schütz, M. (1980). *Bericht über das Forschungsvorhaben Norm-Mess-Silo für Schüttguteigenschaften*. Hochbaustatik, Technische Universität.

Ramírez, A., Nielsen, J., & Ayuga, F. (2010a). On the use of plate-type normal pressure cells in silos. Part 1: Calibration and evaluation. *Computers and Electronics in Agriculture*, *71*(1), 71–76. doi: 10.1016/j.compag.2009.12.004

Ramírez, A., Nielsen, J., & Ayuga, F. (2010b). On the use of plate-type normal pressure cells in silos. Part 2: Validation for pressure measurements. *Computers and Electronics in Agriculture*, *71*(1), 64–70. doi: 10.1016/j.compag.2009.12.005

Ruiz, A., Couto, A., & Aguado, P. J. (2012). Design and instrumentation of a mid-size test station for measuring static and dynamic pressures in silos under different conditions - Part II: Construction and validation. *Computers and Electronics in Agriculture*, *85*, 174–187. doi: 10.1016/j.compag.2012.04.008

Sadowski, A. J., Michael Rotter, J., & Nielsen, J. (2020). A theory for pressures in cylindrical silos under concentric mixed flow. *Chemical Engineering Science*, *223*, 115748. doi: 10.1016/j.ces.2020.115748

Sadowski, A. J., & Rotter, J. M. (2011). Buckling of very slender metal silos under eccentric discharge. *Engineering Structures*, *33*(4), 1187–1194. doi: 10.1016/j.engstruct.2010.12.040

SCHURICHT, T., FÜRLL, C., & ENSTAD, G. G. (2001). Full scale silo tests and numerical simulations of the „cone in cone" concept for mass flow. In *Handbook of Powder Technology* (Vol. 10, pp. 175–180). Elsevier Science BV.

Schwab, C. V, Ross, I. J., White, G. M., & Colliver, D. G. (1994). *WHEAT LOADS AND VERTICAL PRESSURE*. *37*(5), 1613–1619.

Sun, W., Zhu, J., Zhang, X., Wang, C., Wang, L., & Feng, J. (2020). Multi-scale experimental study on filling and discharge of squat silos with aboveground conveying channels. *Journal of Stored Products Research*, *88*, 101679. doi: 10.1016/j.jspr.2020.101679

Sun, Y., & Wang, Y. (2012). Collapse reasons analysis of a large steel silo. *Advanced Materials Research*, *368–373*, 647–650. doi: 10.4028/www.scientific.net/AMR.368-373.647

Teng, B. J. (1994). *PLASTIC COLLAPSE AT LAP JOINTS IN PRESSURIZED CYLINDERS UNDER AXIAL LOAD*. *120*(1), 23–45.

Teng, J. G., & Lin, X. (2005). Fabrication of small models of large cylinders with extensive welding for buckling experiments. *Thin-Walled Structures*, *43*(7), 1091–1114. doi: 10.1016/j.tws.2004.11.006

Teng, J. G., & Rotter, J. M. (1989). Plastic collapse of restrained steel silo hoppers. *Journal of Constructional Steel Research*, *14*(2), 139–158. doi: 10.1016/0143-974X(89)90020-5

Teng, J. G., Zhao, Y., & Lam, L. (2001). Techniques for buckling experiments on steel silo transition junctions. *Thin-Walled Structures*, *39*(8), 685–707. doi: 10.1016/S0263-8231(01)00030-1

Teng, J., & Rotter, J. M. (1991). Collapse Behavior and Strength of Steel Silo Transition Junctions. Part I: Collapse Mechanics. *Journal of Structural Engineering*, *117*(12), 3587–3604. doi: 10.1061/(asce)0733-9445(1991)117:12(3587)

Walker, D. (1967). An approximate theory for pressures and arching in hoppers. *Chemical Engineering Science*, *22*(3), 486. doi: 10.1016/0009-2509(67)80145-3

Walters, J. K. (1973a). A theoretical analysis of stresses in axially-symmetric hoppers and bunkers. *Chemical Engineering Science*, *28*(3), 779–789. doi: 10.1016/0009-2509(77)80012-2

Walters, J. K. (1973b). A theoretical analysis of stresses in silos with vertical walls. *ChemicalEngineering Science*, *28*, 13–21.

Wójcik, M., Tejchman, J., & Enstad, G. G. (2012). Confined granular flow in silos with inserts - Full-scale experiments. *Powder Technology*, *222*, 15–36. doi: 10.1016/j.powtec.2012.01.031

WPMPS. (1989). *Standart Shear Testing Technique for Particulate Solids Using the Jenike Shear Cell“*. England.

Zhao, Y., & Teng, J. G. (2004). Buckling experiments on steel silo transition junctions. II: Finite element modeling. *Journal of Constructional Steel Research*, *60*(12), 1803–1823. doi: 10.1016/j.jcsr.2004.05.001

Zhong, Z., Ooi, J. Y., & Rotter, J. M. (2001). The sensitivity of silo flow and wall stresses to filling method. *Engineering Structures*, *23*(7), 756–767. doi: 10.1016/S0141-0296(00)00099-7